15.1 **LARGE-EDDY SIMULATION OF STREET CANYON FLOW AND POLLUTANT TRANSPORT IN NEUTRAL AND UNSTABLE STRATIFICATIONS**

Wai Chi Cheng, C.-H. Liu* and D. Y. C. Leung
The University of Hong Kong, Hong Kong

1. Introduction

In view of the serious air pollution problems observed in mega cities, the dispersion of air pollutant in urban area has attracted many researchers' attentions in recent decades. Over the past years, vast efforts have been put on the understanding of the flow pattern and pollutant dispersion in street canyons. Different factors, such as building-height-to-street-width (aspect) ratio (Oke 1988), buildings shape (Sagrado et al. 2002; Xie et al. 2005), wind speed (Baik and Kim 1999; Huang et al. 2000) and thermal stability (Nakamura and Oke 1988, Sini et al 1996, Uehara 2000, Kim and Baik 2001, Bohnenstengel et al. 2004, Xie et al. 2006, Cheng et al. 2009, Cai 2009, Li et al. 2009, Park and Baik 2009), have been studied by different parties. For the consideration of the effects of thermal stability, it is generally found that unstable stratification enhances the pollutant removal from street canyons. However, the mechanism of how pollutants are removed in unstable stratification is still unclear. Moreover, previous studies mostly focus on weakly unstable condition (Uehara 2000, Cai 2009, Li et al. 2009). Only very few results considered the scenarios of strongly unstable stratified condition (k-ε model results of Kim and Baik 2001, Xie et al. 2006, Cheng et al. 2009). The limited results from k-ε model suggest that, in unstable condition, both the flow patterns and pollutant removal change significantly.

Because the atmosphere above urban surface is convective most of the time (Roth 2000), thermal stratification is an important parameter for street canyon study. Therefore, a Large-eddy simulation (LES) model is developed to study and compare the flow pattern and pollutant removal in neutral and strongly unstable street canyons (Richardson number Ri = -10). The aim of this study is to improve our understanding of how the mechanisms of flow and pollutant removal change in strongly unstable stratification in street canyons.

2. Numerical model

The LES is performed by the open-source code OpenFOAM (OpenFoam 2009). Mathematical equations of the LES solver "oodles" and the one equation subgrid-scale (SGS) model (Schumann 1975) of the OpenFOAM package are modified for this study to account for buoyancy force.

***** *Corresponding author address*: Liu, Chun-Ho, University of Hong Kong, Department of Mechanical Engineering, Hong Kong. 2859 7901; e-mail: liuchunho@graduate.hku.hk

2.1 *Mathematical equations*

In LES, only the fluctuations with scales larger than the SGS scales can be resolved while the small-scale fluctuations were modeled by the filtering process. In this paper, the resolved-scale quantities are denoted by overline of the variable and SGS quantities are denoted by the subscript $_{SGS}$. The LES model consists of the equation of continuity

$$\frac{\partial \overline{u}_i}{\partial x_i} = 0 \tag{1}$$

and the momentum equation

$$\frac{\partial \overline{u}_i}{\partial t} + \frac{\partial}{\partial x_j}\overline{u}_i\overline{u}_j = -\Delta P\delta_{i1} - \frac{\partial \overline{p}}{\partial x_i} + \left(\frac{1}{\mathrm{Re}_{SGS}} + \frac{1}{\mathrm{Re}}\right)\frac{\partial^2 \overline{u}_i}{\partial x_j \partial x_j} + \alpha g\theta\delta_{i3}. \tag{2}$$

Boussinesq approximation is used for buoyancy. Here u_i is the velocity vector and x_i the spatial coordinates with i=1,2,3. ΔP is the large scale pressure difference, δ_{ij} the Kronecker delta, p the pressure, α the thermal expansion coefficient, g the gravitation acceleration, θ the temperature difference, Re the Reynolds number and Re_{SGS}[=$(C_k k_{SGS}^{1/2}\Delta)^{-1}$] represents the contribution of SGS scales. To solve for the Re_{SGS}, the transport equation for SGS TKE (k_{SGS}) is included

$$\frac{\partial k_{SGS}}{\partial t} + \frac{\partial}{\partial x_i}\left(k_{SGS}\overline{u}_i\right) = \frac{2}{\mathrm{Re}_{SGS}} - C_\varepsilon \frac{k_{SGS}^{3/2}}{\Delta} + \left(\frac{1}{\mathrm{Re}} + \frac{1}{\mathrm{Re}_{SGS}}\right)\frac{\partial^2 k_{SGS}}{\partial x_i \partial x_i} + \frac{\alpha g}{\mathrm{Re}_{SGS}\,\mathrm{Pr}}\frac{\partial \theta}{\partial x_i}\delta_{i3} \tag{3}$$

For temperature and pollutant transports, the transport equations for temperature

$$\frac{\partial \overline{\theta}}{\partial t} + \frac{\partial}{\partial x_i}\overline{u}_i\overline{\theta} = \left(\frac{1}{\mathrm{Re}_{SGS}\,\mathrm{Pr}} + \frac{1}{\mathrm{Re}\,\mathrm{Pr}}\right)\frac{\partial^2}{\partial x_i \partial x_i}\overline{\theta} \tag{4}$$

and pollutant

$$\frac{\partial \overline{c}}{\partial t} + \frac{\partial}{\partial x_i}\overline{u}_i\overline{c} = \left(\frac{1}{\mathrm{Re}_{SGS}\,\mathrm{Sc}} + \frac{1}{\mathrm{Re}\,\mathrm{Sc}}\right)\frac{\partial^2}{\partial x_i \partial x_i}\overline{c} \tag{5}$$

are solved where c is the pollutant concentration. The Spalding's law of the wall (Spalding 1962) was employed for the near-wall treatment. The above equations were solved by the finite volume method (FVM) with second-order-accurate numerical schemes.

2.2 *Simulation parameters*

The Computational domain consists of three two-dimensional (2D) street canyons of unity aspect ratio regularly arranged under the shear layer (Figure 1). Area sources of pollutant and temperature are prescribed on the streets. For horizontal boundaries, the flow and temperature are periodic. However, zero concentration at the inlet and open boundary condition at the outlet are used for the pollutant. All buildings and streets are no-slip. Slip boundary condition with constant temperature is applied at the upper boundary.

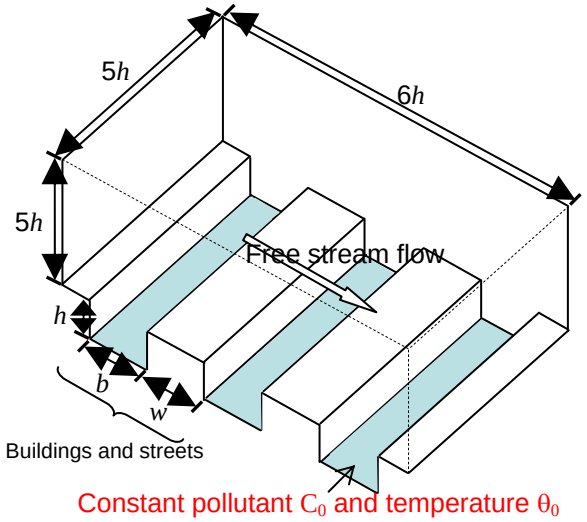

Figure 1. Computation domain.

The Reynolds number is 12,000 and the Richardson numbers Ri (= $\alpha g h \theta_h / U_h^2$) = 0 and -10 are used as the neutral and strongly unstable conditions. Here, θ_h and U_h are, respectively, the temperature and wind speed at the center of street canyon roof level.

The total number of elements are equal to 13.5 million with $N_x \times N_y \times N_z$=50×200×50 elements in the street canyons and $N_x \times N_y \times N_z$=300×200×200 elements in the shear layer where N_i is the number of intervals in the ith direction. The flow statistics were sampled for a time period of $50h/U_f$ with 500 intervals after the initial turbulence activation. In this paper, ensemble average is denoted by <.> while resolved-scale fluctuation by ". Due to the periodic condition for the wind field, its statistics to be presented afterward is further averaged over the three street canyons.

3. Results and Discussions

3.1 *Flow field and pollutant concentration*

For a 2D street canyon of unity aspect ratio in neutral stratification, it is well known that the flow pattern is in the skimming flow regime (Oke 1988). This means that the streamlines of the primary recirculation generated inside street canyon is isolated from those in the shear layer. In neutral condition, the entire primary recirculation locates under the roof level of street canyon. In contrast, in unstable condition, the top of the primary recirculation exceeds the roof level affecting the streamline pattern in the shear layer also (Figure 2). The current LES results show that, in strong unstable condition, the interior of the street canyon is still mostly occupied by the primary recirculation. This is different from the previous k-ε turbulence modeling study (Kim and Baik 2001, Xie et al. 2005, Cheng et al. 2009) where the secondary recirculation is significantly enlarged. For Ri=0, the wind speed is peaked on the windward side. Whereas the wind speed peaked on the leeward side for Ri=-10. It is because the air inside the street canyon is mainly driven by the shear force (at the roof) in neutral condition but is driven by the buoyancy (on the ground) in unstable condition. The momentum is then carried by the primary recirculation into the street canyon on the windward then to the leeward side.

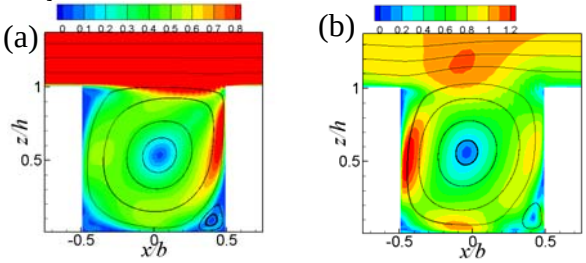

Figure 2. Velocity magnitude $\sqrt{\langle \overline{u}^2 \rangle + \langle \overline{v}^2 \rangle + \langle \overline{w}^2 \rangle} / U_f$ contours and streamlines of (a) Ri=0 and (b) Ri=-10.

The TKE distribution is shown in Figure 3. At the street canyon roof level, The TKE is largest on the windward side in neutral condition but is largest on the leeward side in unstable condition. This is again due to the different mechanisms driving the flow in different stratifications. A sharp peak of TKE is found at the ground-level windward corner in the case of Ri=-10. It could be caused by the secondary recirculation there which traps the hot air. The hot air is unstable so promote the turbulence. Comparing with the result of neutral condition, much higher overall TKE is observed inside the street canyon in unstable condition.

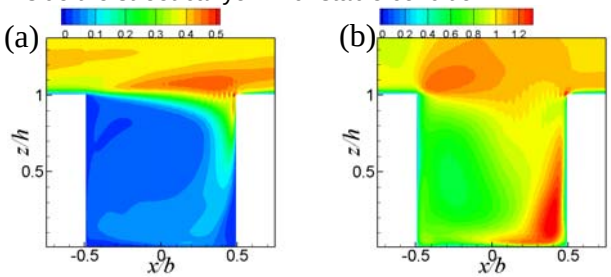

Figure 3. TKE $[\langle u"u" \rangle + \langle v"v" \rangle + \langle w"w" \rangle) / U_f^2]$ contours of (a) Ri=0 and (b) Ri=-10.

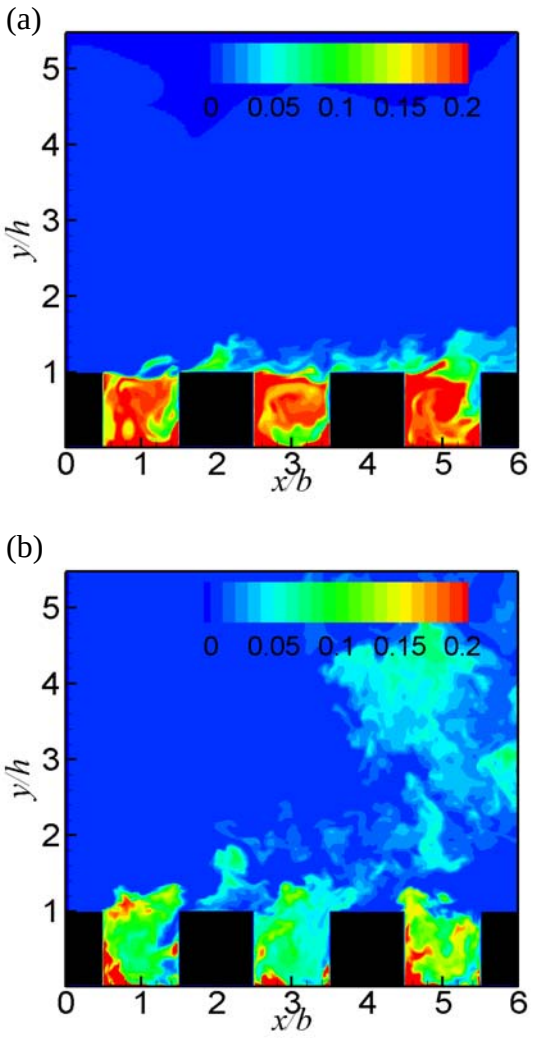

Figure 4. Snapshot of pollutant concentrations of (a) Ri=0 and (b) Ri=-10.

The instantaneous pollutant concentration on the vertical center-plane in neutral and unstable conditions are compared in Figure 4. In neutral condition, the pollutant is well mixed by the primary recirculation inside the street canyon. The pollutant removal and the fresh air entrainment occur mainly on the windward side. Moreover, the pollutant being removed to the shear layer only stays in a shallow layer above the buildings.

However, in unstable condition, the strong buoyancy force changes the pollutant removal mechanism a lot. The pollutant is then able to escape from the street canyon on the leeward side. The pollutant concentration is thus not as uniform as that in neutral condition. Moreover, the pollutant now becomes able to disperse into the upper level of the shear layer.

The more effective pollutant removal in the unstable conditions also implies the lower average pollutant concentration inside the street canyons. From the current two sets of calculations, the pollutant concentration in unstable conditions is about one half of that in the neutral conditions (Table 1).

Table 1. Average pollutant concentration/C_0.

	1st canyon	2nd canyon	3rd canyon
Ri = 0	0.200	0.216	0.226
Ri = -10	0.116	0.120	0.126

3.2 *Momentum and pollutant exchanges*

Street canyon exchanges momentum and pollutant with shear layer through the street canyon roof. Large differences in both the vertical momentum flux $\langle u''w''\rangle$ and vertical pollutant flux $\langle w''c''\rangle$ are observed between the results of Ri = 0 and Ri = -10 (Figure 5). In neutral conditions, $\langle u''w''\rangle$ is negative in most region of the street canyon roof suggesting that streamwise momentum is transferred from the shear layer into the street canyon. However, in unstable conditions, $\langle u''w''\rangle$ is positive in most of region instead and peaked at the leeward side. This means that momentum generated by buoyancy is transferred from the street canyons upward to the shear layer. In other words, the street canyons becomes sources of energy production.

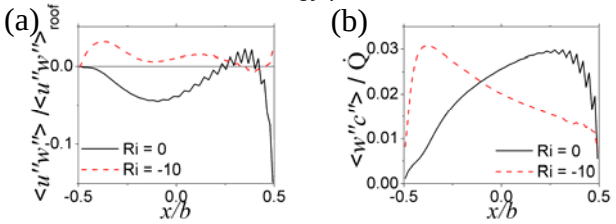

Figure 5. Profiles of (a) $\langle u''w''\rangle / \langle u''w''\rangle_{roof}$ and (b) $\langle w''c''\rangle / U_f Q$ along street canyon roof where $\langle u''w''\rangle_{roof}$ and Q are the roof level average of momentum flux and pollutant flux.

Shift in the peak location of $\langle w''c''\rangle$ is also observed (Figure 5b). As Ri changes from 0 to -10, the key pollutant removal location shifts from the windward side to the leeward side. The pattern of the vertical pollutant flux at the street canyon roof generally agrees with our previous k-ε model result (Cheng et al 2009).

Table 2. Definitions of quadrants.

	$\langle u''w''\rangle$	$\langle w''c''\rangle$
Ejection	$u''<0, w''>0$	$w''>0, c''>0$
Outward interactions	$u''>0, w''>0$	$w''>0, c''<0$
Sweeps	$u''>0, w''<0$	$w''<0, c''<0$
Inward interactions	$u''<0, w''<0$	$w''<0, c''>0$

In order to investigate the roof-level $\langle u''w''\rangle$ and $\langle w''c''\rangle$ in details, the method of quadrant analysis is employed where $\langle u''w''\rangle$ and $\langle w''c''\rangle$ are divided into four components according to the signs of u'', w'' and c'' (Table 2). Moreover, the roof level of the street canyon

is also divided into five sections depending on the location along the roof for a more detailed investigation.

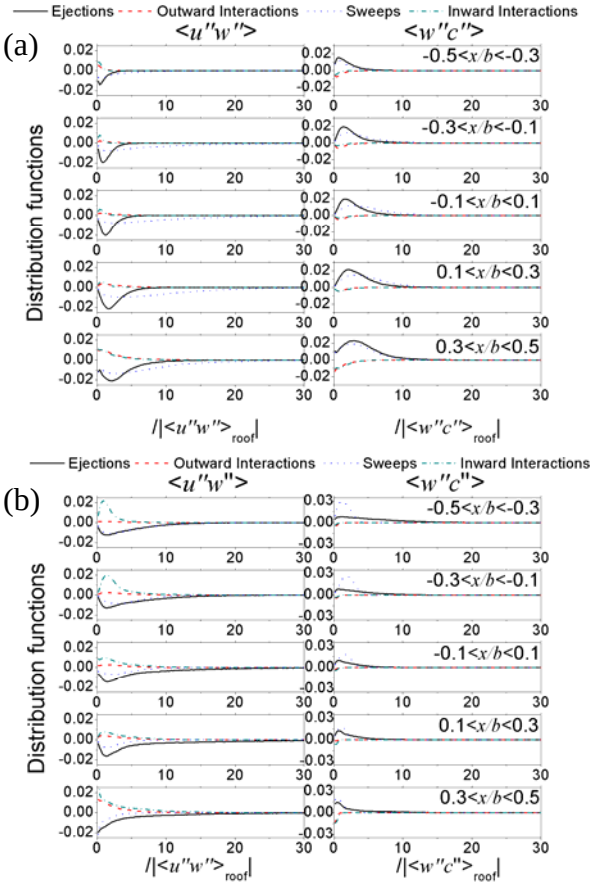

Figure 6. Quadrant analysis for $\langle u''w''\rangle$ and $\langle w''c''\rangle$ of (a) Ri=0 and (b) Ri=-10.

The contributions of individual quadrants to the total fluxes are calculated by conditional sampling. Figure 6 shows the distribution functions of the quadrants in the five regions with respect to the magnitude of the event. In neutral condition, both $\langle u''w''\rangle$ and $\langle w''c''\rangle$ are mostly contributed by ejections and sweeps while inward and outward interactions are insignificant. The distribution functions of sweeps and ejections show nearly the same pattern and shape. while moving from leeward side to the windward side, both the magnitudes and scales of the events increase. Therefore, most of the momentum and pollutant exchanges occurred on the windward side in neutral conditions are facilitated by large-scale fluctuations.

Different patterns for $\langle u''w''\rangle$ and $\langle w''c''\rangle$ are observed in the unstable conditions. For $\langle u''w''\rangle$, inward and outward interactions, which represent the upward transfer of momentum, become important. Especially, inward interactions become the dominated quadrant on the leeward side. On the windward side, similar distributions for the inward and outward interactions are observed which are offset by the sweeps and ejections. For pollutant removal, sweeps and ejections are still the dominated events since the pollutant is removed from the street canyon to the shear layer. Different from the result of neutral conditions, the largest pollutant flux is observed on the leeward side which is driven mainly by sweeps. For Ri = -10, the scales of the events are larger on the leeward side than those on the windward side. These all are caused by the turbulence generated by the buoyancy force as a result of ground heating.

3.3 *Roof-level averaged quantities*

Table 3. Roof-level Averaged turbulent quantities.

Ri	σ_u/U_f	σ_v/U_f	σ_w/U_f	$\langle u''w''\rangle_{roof}$ / U_f^2	$\langle w''c''\rangle_{roof}$ / U_fC_0
0	9.42 $\times10^{-2}$	5.71 $\times10^{-2}$	5.23 $\times10^{-2}$	-2.79 $\times10^{-3}$	2.14 $\times10^{-3}$
-10	5.25 $\times10^{-1}$	4.98 $\times10^{-1}$	5.92 $\times10^{-1}$	-8.14 $\times10^{-2}$	2.58 $\times10^{-2}$

The average values of the velocity standard deviations (σ_u, σ_v, σ_w), vertical momentum flux ($\langle u''w''\rangle$) and vertical pollutant flux ($\langle w''c''\rangle$) at the street canyon roof level are calculated (Table 3). In unstable conditions, all quantities calculated are larger than that of the neutral conditions by an order of magnitude. The increases in velocity standard deviations signify the increases in TKE production in unstable conditions. Moreover, σ_w is directly related to the exchange of air between the street canyon and the shear layer. Compare with the previous k-ε model study about the air exchange rate (ACH, Cheng et al. 2009), the observed increment of air exchange in unstable conditions is much larger in the current LES result. This may due to the under-estimation of the turbulence in k-ε model. In addition, the current results also suggest the significant enhancement of momentum and pollutant exchange in unstable conditions.

4. Conclusions

In this paper, the flow pattern and pollutant removal in neutral (Richardson number (Ri = 0)) and strongly unstable (Ri = -10) conditions are investigated by large-eddy simulation (LES).

In neutral condition, the momentum and pollutant exchanges occur mostly on the windward side. This is a result of the instability developed at the street canyon roof due to the large velocity gradient. The perturbed flow then travels and develops along the street canyon roof, and finally impinges the windward facades. Turbulence is then produced then in turn promotes the momentum and pollutant exchanges near the roof-level windward facade.

In strongly unstable conditions, the momentum and pollutant exchanges are governed by another different mechanism. As ground heating is switched on that increases the buoyancy force. The air is heated up near the ground level that follows the primary recirculation moving to the leeward side. For Ri = -10, the buoyancy force is strong enough that the air sometime able to penetrate the roof level that transfers both momentum and pollutant to the shear layer directly near the leeward facade.

As a result, major locations of momentum and pollutant removal switched from the windward side to the leeward side once the thermal stratification changes from neutral to strongly unstable. At the same time, the increases in TKE, and vertical momentum and pollutant fluxes are larger than its unstable counterpart by another of magnitude. The current results therefore suggested the completely different mechanisms of the momentum exchange and pollutant removal in neutral and unstable conditions. More analyses are thus necessary for the thorough understanding of the flow and pollutant removal behaviors in low Ri.

5. References

Baik, J.-J., Kim, J.-J., 1999: A numerical study of flow and pollutant dispersion characteristics in urban street canyons. Journal of Applied Meteorology, 38, 1576-1589.

Bohnenstengel, R., Plamgren, F., Hertel, O., Vignati, E., 1996: Using measurements of air pollution in streets for evaluation of urban air quality-meteorological analysis and model calculations. The Science of the Total Environment, 189, 259-265.

Cai, X., 2009: Differential wall heating in street canyons: Flow characteristics. Proceeding of the 7th International Conference on Urban Climate ICUC-7, Yokohama, Japan, 29/6-3/7, 2009.

Cheng, W.C., Liu, C.H., Leung, D.Y.C., 2009: On the correlation of air and pollutant exchange for street canyons in combined wind-buoyancy-driven flow. Atmospheric Environment, 43, 3682-3690.

Huang, H., Akutsu, Y, Arai, M, Tamura, M., 2000: A two-dimensional air quality model in an urban street canyon: evaluation and sensitivity analysis. Atmospheric Environment, 34, 689-698.

Kim, J.J., Baik, J.J, 2001: Urban street-canyon flows with bottom heating. Atmospheric Environment, 35, 3395-3404.

Li, X.X., Koh, T.Y., Britter, R., Liu, C.H., Norford, L.K., Entekhabi, D., Leung, D.Y.C., 2009: Large-eddy simulation of flow field and pollutant dispersion in urban street canyons under unstable stratification. Proceeding of the 7th International Conference on Urban Climate ICUC-7, Yokohama, Japan, 29/6-3/7, 2009.

Nakamura,Y., Oke,T.R., 1988: Wind, temperature and stability conditions in an east-west oriental urban canyon. Atmospheric Environment, 22, 2691-2700.

OpenFoam, 2009: http://www.opencfd.co.uk/openfoam/.

Oke, T.R., 1988: Street design and urban canopy layer climate. Energy and Building, 11, 103-113.

Park, S.B., Baik, J.J., 2009: LES study of thermal effects on turbulent flow and dispersion in a street canyon. Proceeding of the 7th International Conference on Urban Climate ICUC-7, Yokohama, Japan, 29/6-3/7, 2009.

Sagrado, A.P.G, Beeck, J.V., Rambaud, P., Olivari, D., 2002: Numerical and experimental modeling of pollutant dispersion in a street canyon. Journal of Wind Engineering and Industrial Aerodynamics, 90, 321-339.

Schumann, U., 1975: Subgrid scale model for finite difference simulations of turbulent flows in plane channels and annuli. Journal of Computational Physics, 18, 376-404.

Sini, J.F., Anquetin, S., Mestayer, P.G., 1996: Pollutant dispersion and thermal effects in urban street canyons. Atmospheric Environment 30, 2659-2677.

Spalding, D.B., 1962: A new analytical expression for the drag of a flat plate valid for both the turbulent and laminar regimes. Journal of Heat and Mass Transfer 5, 1133-1138.

Uehara, U., Murakami, S., Oikawa, S., Wakamatsu, S., 2000: Wind tunnel experiments on how thermal stratification affects flow in and above urban street canyons. Atmospheric Environment 34, 1553-1562.

Xie, X., Huang, Z., Wang, J., Xie, Z., 2005: The impact of solar radiation and street layout on pollutant dispersion in street canyon. Building and Environment, 40, 201-212.

Xie, X., Liu, C.H., Leung, D.Y.C., Leung, M.K.H., 2006: Characteristics of air exchange in a street canyon with ground heating. Atmospheric Environment, 40, 6396-6409.